A Simple Model of Cross-Flow Filtration Based on Particle Adhesion

K. Stamatakis and Chi Tien
Dept. of Chemical Engineering and Materials Science, Syracuse University, Syracuse, NY 13244

A simple model presented for cross-flow filtration of liquid suspensions was formulated on the premise that among the particles convected to the filter medium surface in cross-flow filtration, only a fraction of them become deposited. A criterion based on the interplay of the geometry of the cake-suspension interface and various forces acting on a particle as it moves toward the interface was established and an expression of the adhesion probability of impacting particles developed. The model was then formulated by incorporating the adhesion probability information together with conventional cake filtration theories. Through sample calculations, the model was found to display behavior consistent with the observed phenomena of cross-flow filtration and capable of representing experimental results.

Introduction

Cross-flow filtration refers to a type of surface filtration in which the main direction of the suspension flow is perpendicular to the flow direction of the recovered (or separated) liquid. The term "cross-flow" describes the flow pattern and does not specify the type of media used for particle retention. Consequently, a number of processes such as reverse osmosis, ultrafiltration, and microfiltration may be classified as cross-flow filtration. On a more restricted basis, cross-flow filtration is usually considered a process for removing particles ranging in size from 0.1 to 10.0 μm from relatively dilute suspensions using polymeric or metallic media (or membranes) with defined pore size. It is commonly applied to clarify dilute suspensions of fine particles for producing filtrates of high purity.

In cross-flow filtration, the suspension to be treated flows under pressure along a porous medium (or membrane) with liquid permeation taking place across the membrane. As liquid permeates the medium, a portion of the particles associated with the permeating liquid's flow deposits at the surface of the medium to form a solid cake. The cake thickness increases with time and as a result, the rate of liquid permeation decreases with time. This time-dependent behavior represents a major characteristic of cross-flow filtration.

A number of investigators have previously proposed models for cross-flow filtration. For all these models, the one central issue in analyzing cross-flow filtration is: How does one estimate the fraction of particles transported to the membrane surface associated with the permeating liquid become deposited? If one assumes that all particles are deposited, then the cake thickness (and its resistance to liquid flow) would be so great that it would lead to a liquid flux at least one order of magnitude less than what is observed experimentally. The problem of modeling, therefore, is to suggest a physically plausible hypothesis for explaining the fact that only a fraction of the particles transported to the medium surface become deposited and form a cake.

Some of the early work on modeling cross-flow filtration (Blatt et al., 1970; Porter, 1972; Henry, 1972) recognized the similarities in flow pattern between cross-flow filtration and reverse osmosis. This recognition led to the use of the concentration polarization model of reverse osmosis in correlating and interpreting experimental data of cross-flow filtration. This attempt, however, was largely unsuccessful since it tends to grossly underpredict the permeation flux (by one or two orders of magnitude). The failure was attributed to the use of the Stokes-Einstein equation for estimating particle diffusivity. In order to overcome this difficulty, Altena and Belfort (1984) suggested the inclusion of a lateral migration of particles in considering the back diffusion of particles from membrane surfaces. This modification, however, did not significantly improve the agreement between experiments and predictions.

Another attempt to model cross-flow filtration using the concentration-polarization model was suggested by Zydney (1985) and Zydney and Colton (1986). Instead of using the

Present address of K. Stamatakis: 12 Magnisias St., Thive 32200, Greece.

Stokes-Einstein particle diffusivity to account for the back-diffusion of particles, Zydney and Colton used the so-called shear-induced particle diffusivity and obtained agreement between prediction and their experimental data of membrane plasmapheresis.

More recently, Davis and coworkers (Davis and Birdsell, 1987; Davis and Leighton, 1987; Romero and Davis, 1988, 1990) analyzed cross-flow filtration on the basis of shear-induced particle diffusion. Both steady-state and transient-state analyses were made. As shown in the more recent work of Romero and Davis (1990), it was assumed that particle transport toward the membrane surface due to liquid permeation results in the formation of a "stagnation cake" layer and a "flowing cake" layer, the thickness of both increasing longitudinally. The model predicts liquid permeation flux to be a function of the longitudinal distance and time. There is no direct experimental observation about the presence of such entities nor their physical structure and properties can be independently measured.

The purpose of the present work is to present a model for cross-flow filtration based on particle adhesion instead of particle back-diffusion or motion. Both Fischer and Raasch (1986) and Lu and Ju (1989) presented experimental evidence that in cross-flow filtration, among the particles transported to the membrane surface, only a fraction become deposited. Thus, by developing a criterion for estimating the value of the fraction of particles deposited and combining the criterion with conventional cake filtration theories, one can readily predict the extent of decline of local liquid flux with time as well as the size distribution of particles that form the growing solid cake. The model presented in this study is formulated on such a basis.

Criterion for Particle Adhesion

Fischer and Raasch (1986) and Lu and Ju (1989) observed in their respective experimental studies of cross-flow filtration the formation of immobile cakes along the upstream side of the membrane medium. Furthermore, they found that particles that formed the cake came from the smaller particles present in the suspension and that higher cross-flow velocities resulted in cake composed of finer particles. Fischer and Raasch suggested a qualitative model for estimating the selective cut-diameter of deposited particles. On the other hand, Lu and Ju present a criterion for selective particle deposition based on the hydrodynamic forces acting on a particle touching the membrane medium surface and the angle of repose between the particle and the surface. The model presented below is a generalization and quantification of these concepts.

A schematic diagram depicting a spherical particle of diameter d_p transported to the vicinity of the cake-suspension interface with a protrusion of finite height, h, is shown in Figure 1. [The protrusion may be considered one of the deposited particles. Thus, the criterion developed, strictly speaking, is not applicable to a clean membrane or the initial period of cross-filtration. On the other hand, since this initial period is relatively short (as shown by the observed rapid flux decline), it may be ignored.] The forces acting on the particle are F_p (along the direction of the main flow) and F_q (along the direction of permeation). The condition for deposition (that is, the particle remains static) is:

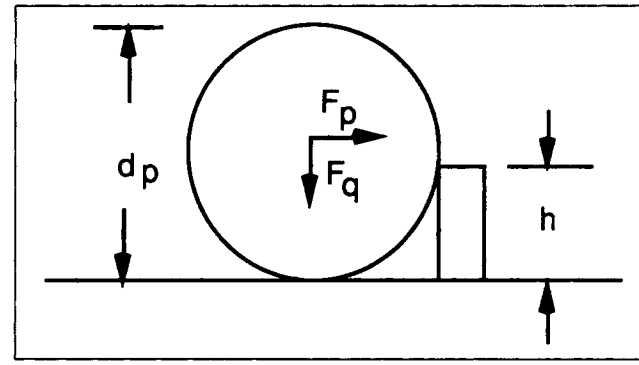

Figure 1. Forces acting upon a spherical particle in contact with the cake surface.

$$F_q\sqrt{\left(\frac{d_p}{2}\right)^2-\left(\frac{d_p}{2}-h\right)^2}\geq F_p\left(\frac{d_p}{2}-h\right) \tag{1}$$

or

$$h\geq\left(1-\frac{1}{\sqrt{(F_p/F_q)^2+1}}\right)\frac{d_p}{2} \tag{2}$$

In other words, for deposition to occur, a particle must be placed next to a protrusion of sufficient height. The minimum height can be obtained from the above relationship, namely,

$$h_{\min}=\left(1-\frac{1}{\sqrt{(F_p/F_q)^2+1}}\right)\frac{d_p}{2} \tag{3}$$

The type of forces acting on a spherical particle in contact with the suspension/cake interface vary with the size of the particle and may include the hydrodynamic force, the gravitational force, the surface interaction forces and the diffusional force. The diffusional force is important primarily for submicron particles. The surface interaction forces, in the context of cross-flow filtration are the double layer and Van der Waals forces, which depend strongly on the thickness of the liquid film (that is, separation distance) between the particle and membrane surface (or the particles themselves). Since this thickness value is unknown and furthermore both of these two forces are shortranged, these forces will be ignored in the following considerations.

A first step toward estimating the forces involved is to describe the flow field near the suspension/cake interface, as depicted in Figure 2. In the immediate neighborhood of the slurry/cake interface, the velocity field may be approximated as:

$$w=\frac{\tau_w}{\mu}\cdot y \tag{4}$$

where y is the distance from the cake/slurry interface, τ_w is the shear stress acting on the suspension/cake interface and μ is the liquid viscosity.

According to O'Neill (1968), the drag force exerted on a single spherical particle in a shear flow field as shown in Figure 2 is:

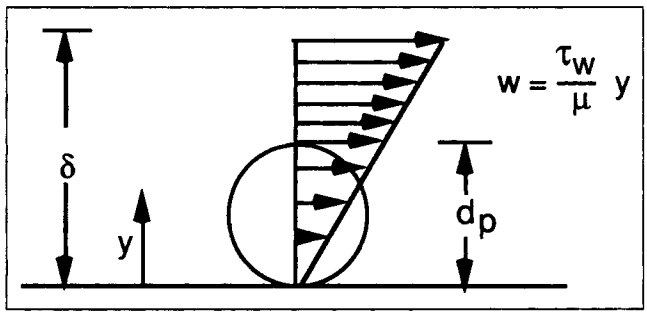

Figure 2. Spherical particle in contact with the cake surface in a shear flow.

$$F_p = 1.7009 \left[3\pi\mu d_p w \Big|_{y=d_p/2} \right] \tag{5}$$

Next, consider the various forces acting on the particle along the y-direction. The hydrodynamic drag force exerted on the particle by the permeating liquid, F_q, is:

$$F_{q1} = 3\pi\mu d_p v_w \tag{6}$$

where v_w is permeation flux (or velocity).

For a neutrally buoyant spherical particle in a simple shear flow field, Vasseur and Cox (1976) have shown that the lateral migration velocity is given as:

$$u_L = \frac{61}{576\nu}\left(\frac{\tau_w}{\mu}\right)^2\left(\frac{d_p}{2}\right)^3 \tag{7}$$

where ν is the kinematic viscosity of the liquid.

Strictly speaking, the above expression is valid for the channel Reynolds number less than 15. More accurate expressions (Schonberg and Hinch, 1989; Drew et al., 1991) for large Reynolds numbers are available. The use of these expressions, however, requires rather tedious computation. As a matter of simplification, Eq. 7 is used as a conservative estimation.

The lateral lift force acting on the particle, F_{q_2}, is:

$$F_{q2} = 3\pi\mu d_p u_L \tag{8}$$

On the other hand, the buoyant force of the spherical particle, F_{q_3}, is:

$$F_{q3} = \frac{\pi}{6}(\rho_s - \rho_l) g\, d_p^3 \tag{9}$$

where ρ_s and ρ_l are the particle and liquid densities. Consequently, the net force acting on the particle along the y-direction, F_q, is:

$$F_q = F_{q1} - F_{q2} + F_{q3}$$

or

$$F_q = 3\pi\mu d_p (v_w - u_L) + \frac{\pi}{6}(\rho_s - \rho_l) g d_p^3 \tag{10}$$

Both Eqs. 5 and 10, which give the expressions of F_p and F_q, respectively, include the wall shear stress, τ_w, which can be calculated from the friction factor correlation, or

$$f = \frac{2\tau_w}{\rho_l w_s^2} = \begin{cases} 24/\mathrm{Re} & \text{for laminar flow} \\ 0.073\ \mathrm{Re}^{-1/4} & \text{for } 6.0.10^3 \le \mathrm{Re} \le 6.0.10^5 \end{cases} \tag{11}$$

where Re is the Reynolds number, defined as $d\rho_l w_s/\mu$ where d is the diameter (or equivalent diameter) of the membrane channel. In terms of the friction factor, F_p and F_q become:

$$F_p = 1.276\ \pi\rho_l d_p^2 f w_s \tag{12}$$

$$F_q = 3\pi\mu d_p v_w - 0.01\pi\mu\frac{f^2 w_s^4 d_p^4}{3} + \frac{\pi}{6}(\rho_s - \rho_l) g d_p^3 \tag{13}$$

The values of the minimum protrusion height for particle deposition, $h_{\min}$, can be calculated by substituting the above expressions of F_p and F_q into Eq. 3. $h_{\min}$ is a function of the cross-flow velocity, w_s, the permeation flux, v_w, the particle diameter, d_p, and the properties of both the liquid and the particles. The values of $h_{\min}$ as a function of d_p for different operating conditions are shown in Figures 3 and 4 with the properties of the particles and liquid used in the calculations listed in Table 1. In Figure 3, the values of $h_{\min}$ were plotted vs. d_p for different cross-flow velocities at constant permeation flux. Figure 4, on the other hand, gives the values of $h_{\min}$ vs. d_p for various values of permeation flux with w_s being constant. Both figures show that the value of $h_{\min}$ increases with the increase in particle size. On the other hand, increasing cross-flow velocity or decreasing permeation flux increases the $h_{\min}$ required for particle deposition.

Particle Adhesion Probability

As shown in Figures 3a and 3b, the minimum protrusion height for particle deposition, $h_{\min}$, varies with both the operating conditions and particle diameter. The protrusion height at a suspension/cake interface can be expected to cover a range of values. For a given particle transported to the suspension/cake interface, its deposition depends upon the height of the protrusion with which the particle comes into contact. Assuming that the protrusion height is a continuous random variable with a continuous distribution function, the probability for a spherical particle of diameter d_p to be deposited at the cake surface equals the probability for a local protrusion height to be greater than or equal to $h_{\min}$, $P(h \ge h_{\min})$, in other words,

$$\gamma = P(h \ge h_{\min}) = 1 - P(h \le h_{\min}) \tag{14}$$

where γ is the probability for a spherical particle to be deposited at the membrane surface, or its adhesion probability. For a population of particles transported to the membrane surface in cross-flow filtration, the adhesion probability may be taken as the fraction of the population of particles which become deposited. The adhesion probability depends on the protrusion height density distribution. As an approximation, if one assumes that the protrusion height follows a uniform distribution over $0 \le h \le h_{\max}$, where $h_{\max}$ is the maximum protrusion height, then Eq. 14 becomes:

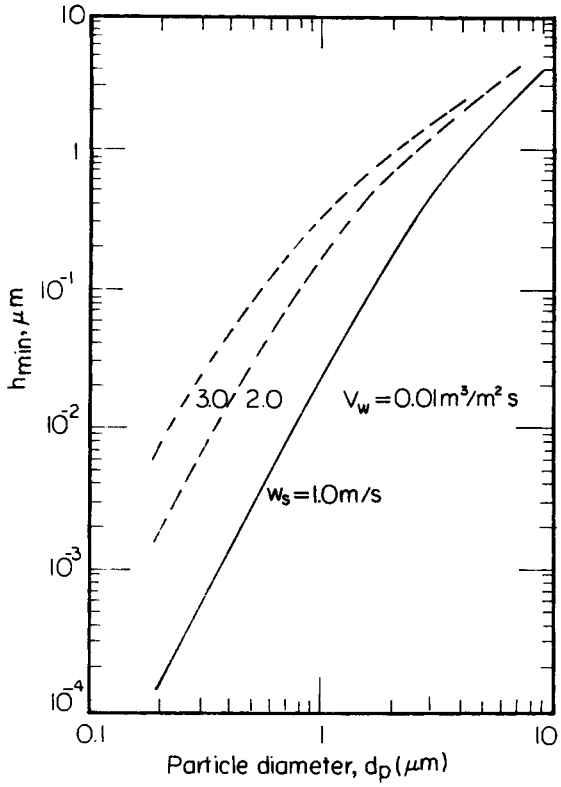

Figure 3a. Minimum protrusion height vs. particle size for different operating conditions.

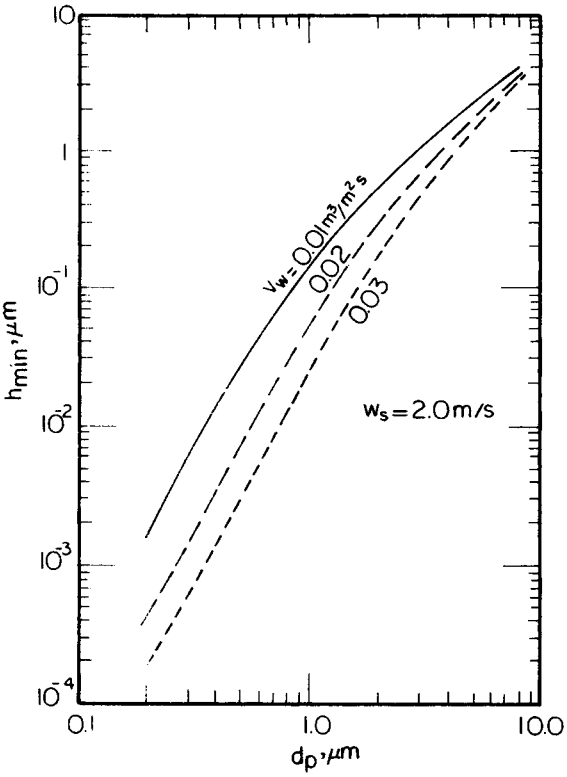

Figure 3b. Minimum protrusion height vs. particle size for different operating conditions.

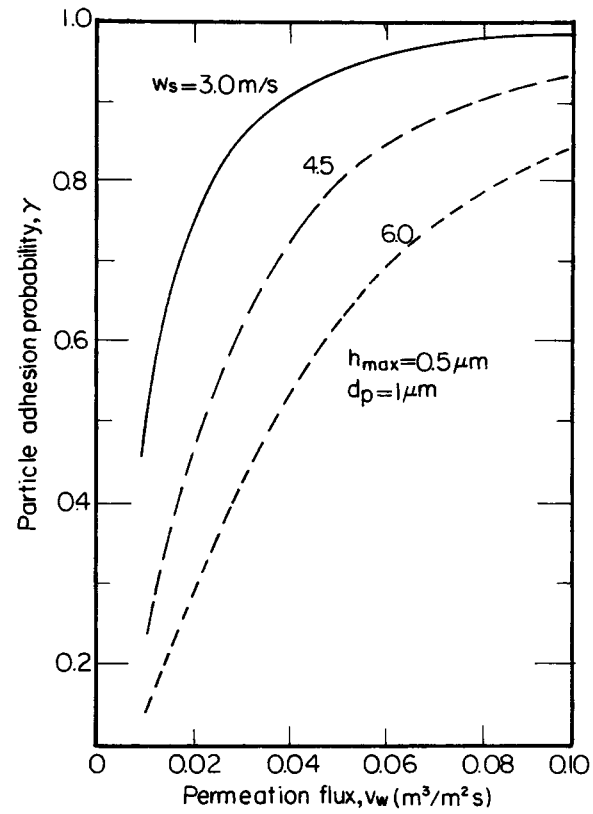

Figure 4. Particle adhesion probability vs. permeation flux for various cross-flow velocities.

$$P(h \le h_{min}) = \frac{h_{min}}{h_{max}} \tag{15}$$

Substituting Eq. 3 into the above expression, one has:

$$\gamma = 1 - \left[1 - \frac{1}{\sqrt{(F_p/F_q)^2 + 1}}\right] \frac{d_p}{2h_{max}} \tag{16}$$

Suspensions to be treated by cross-flow filtration are likely to be polydispersed. The fraction (volume-based) of the total population of particles transported to the medium surface achieving deposition can be found from the size distribution of the total population of particles and the adhesion probability of particles of different sizes. Let c_i denote the volume fraction of particles of diameter d_{p_i}, $i = 1,2 \ldots N$, present in the sus-

Table 1. Physical Properties of Suspensions and Cakes Used in Adhesion Probability and Sample Calculations

Parameters	Values
ϵ_{so}	0.002
d_p^*	1 μm
ρ_l	1,000 kg/m^3
ρ_s	2,600 kg/m^3
μ	0.001 Pa·s
$\epsilon_s = \epsilon_s^o$	0.250
$k = k_o$	$1.00 \cdot 10^{-14}$ m^2
L_o	10^{-4} m

*Not applicable to those cases where d_p is considered a variable.

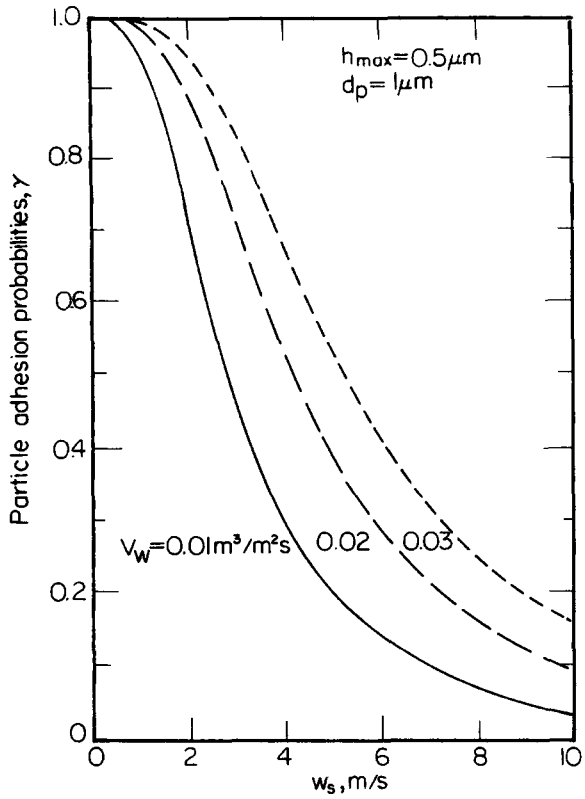

Figure 5. Particle adhesion probability vs. cross-flow velocity for various permeation fluxes.

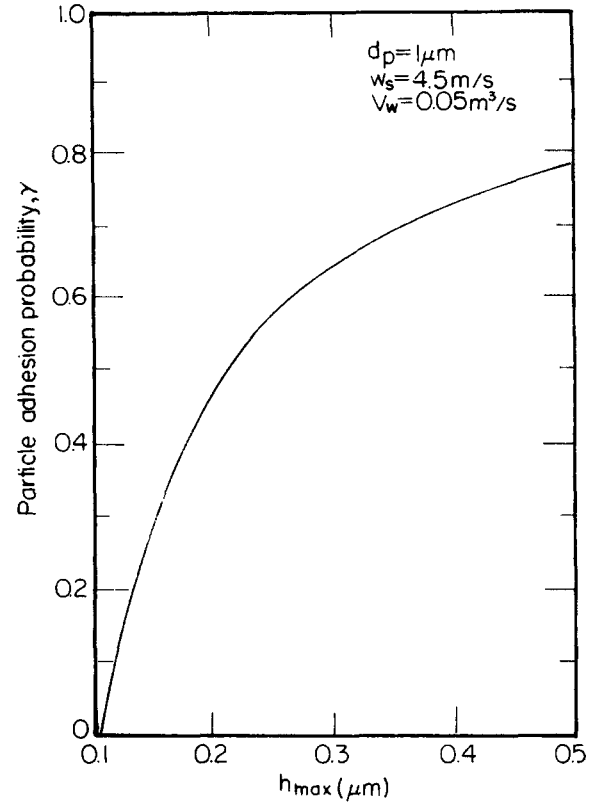

Figure 6. Particle adhesion probability vs. the upper limit of the uniform distribution, h_{max}.

pension and γ_i be the corresponding adhesion probability. The volume fraction of the total particles achieving deposition, $\bar{\gamma}$, is:

$$\bar{\gamma} = \frac{\sum_{i=1}^{N} c_i \gamma_i}{\sum_{i=1}^{N} c_i} \tag{17}$$

Equations 16 and/or 17 together with Eqs. 12 and 13 can be used to estimate the fraction of the particles which are transported to the medium surface and become deposited to form a cake. For a given set of operating conditions in cross-flow filtration, the value of γ decreases as the permeation flux, v_w, declines. On the other hand, since the permeation flux decreases with increasing cake thickness, one may expect γ to be a monotonically decreasing function of time. This behavior implies that one may expect v_w to decline with time but with a diminishing declining rate, which is indeed observed experimentally in cross-flow filtration (Fischer and Raasch, 1986; Lu and Ju, 1989).

The adhesion probability can also be seen to be a monotonically decreasing function of the particle diameter, d_p. Accordingly, among the particles deposited, smaller-particle enrichment characterizes the deposition as compared with the total population of particles transported. This feature has also been observed experimentally (Fischer and Raasch, 1986; Murkes and Carlsson, 1988).

To calculate γ, one must know the value of the maximum protrusive height, h_{max}. Although there is no precise method of determining h_{max}, one may argue on physical ground that h_{max} should be of the same order of magnitude of the size of the deposited particles. Thus, one may assume $h_{max} = d_p/2$ for monodispersed suspension and $h_{max} = \bar{d}_p/2$ for polydispersed suspensions where $\bar{d}_p$ is the volume mean diameter.

Quantitatively, the effect of the various variables (namely, w_s, v_w, d_p, and h_{max}) are shown in Figures 4 through 7. In Figure 4, γ is shown as a function of v_w for different values of w_s for particles of 1 μm diameter. Similarly, in Figure 5, γ is plotted against w_s for three different values of v_w. The results demonstrate that increasing w_s or decreasing v_w decreases γ. On the other hand, when the operating variables are kept constant while the surface roughness increases, the particles adhesive probability increases (see Figure 6). In Figure 7, γ is shown to be a monotonically decreasing function of d_p under different conditions.

The size distribution of the deposited particles estimated according to the adhesion probability concept discussed above is shown in Figure 8. Let x_i denote the volume fraction of the total population of particles in a suspension with particles of diameter d_{p_i}, $i = 1, \ldots N$, and γ_i the corresponding adhesion probability. Then, the volume fraction of particles of d_{p_i} present in the cake formed from the suspension, y_i, is:

$$y_i = \frac{x_i \gamma_i}{\sum_{j=1}^{N} x_j \gamma_j} \tag{18}$$

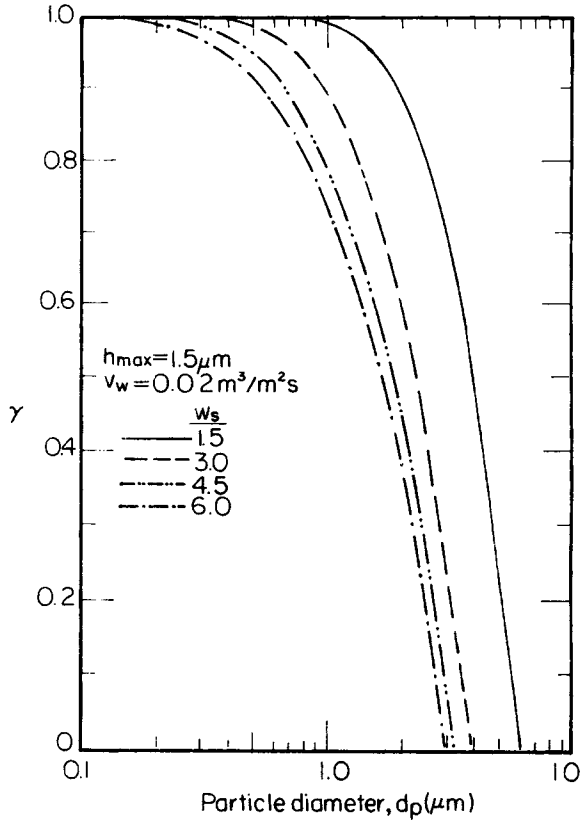

Figure 7a. Particle adhesion probability vs. particle size for different operating conditions.

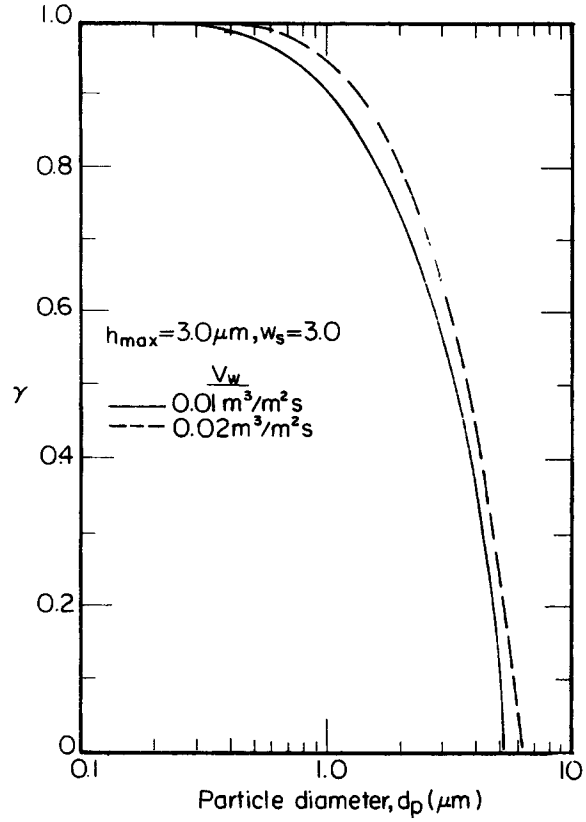

Figure 7b. Particle adhesion probability vs. particle size for different conditions.

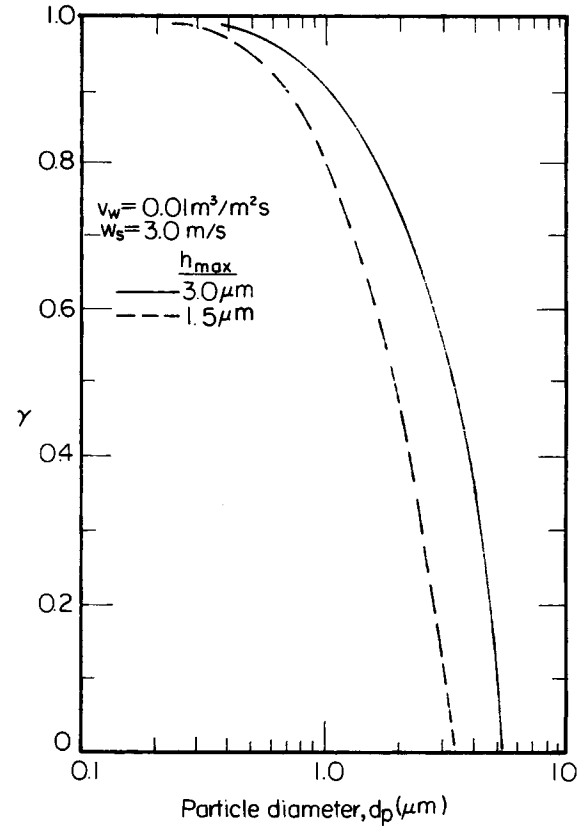

Figure 7c. Particle adhesion probability vs. particle size for different operating conditions.

The results shown in Figure 8 were calculated according to the above expression. A normal distribution was assumed for the total population of particles in the suspension, with a mean diameter of 5 μm and a standard deviation of 1 μm. The enrichment of finer particles in cake formation is clearly demonstrated in this figure. The size distribution of the deposited particle varies with the operating condition. But in all cases, the cake particles are finer than those of the total population, with the degree of fineness increasing with the magnitude of v_w.

Cross-Flow Filtration Model

Over the past five decades, considerable effort has been devoted to studying cake filtration and modeling cake-filtration processes. By incorporating the adhesion probability results with anyone of the existing cake-filtration models, one may readily predict the performance of cross-flow filtration. In the following, we present a cross-flow filtration model based on the assumption that the cake formed is incompressible or is compressible but may be characterized by its average properties.

A schematic representation of cake formation is shown in Figure 9. The dynamic behavior of cross-flow filtration is a function of both the time and spatial variables. The spatial dependence is, however, rather weak (or v_w is nearly independent of the axial distance) unless the axial distance involved is exceedingly large. In the formulation given below, for reasons of simplification, the spatial dependence is ignored. (The

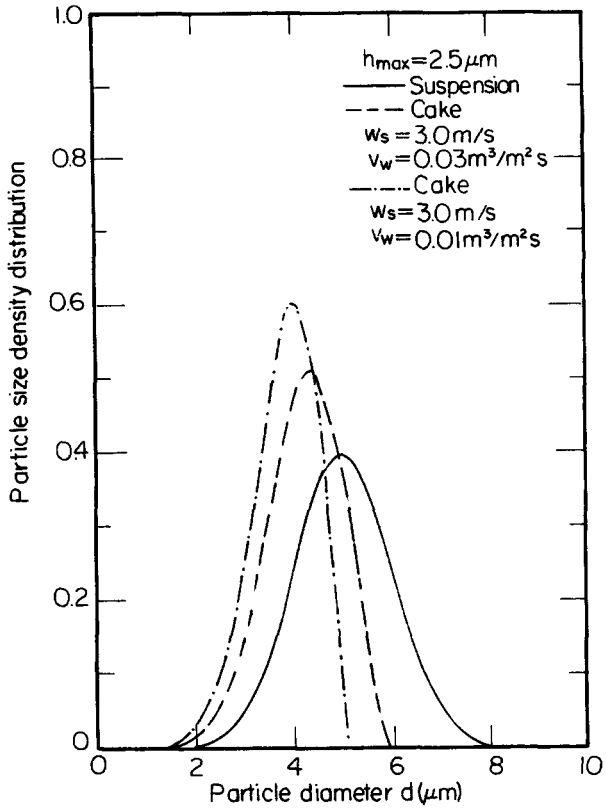

Figure 8a. Size distribution functions of suspended particles and cake particles permeation fluxes.

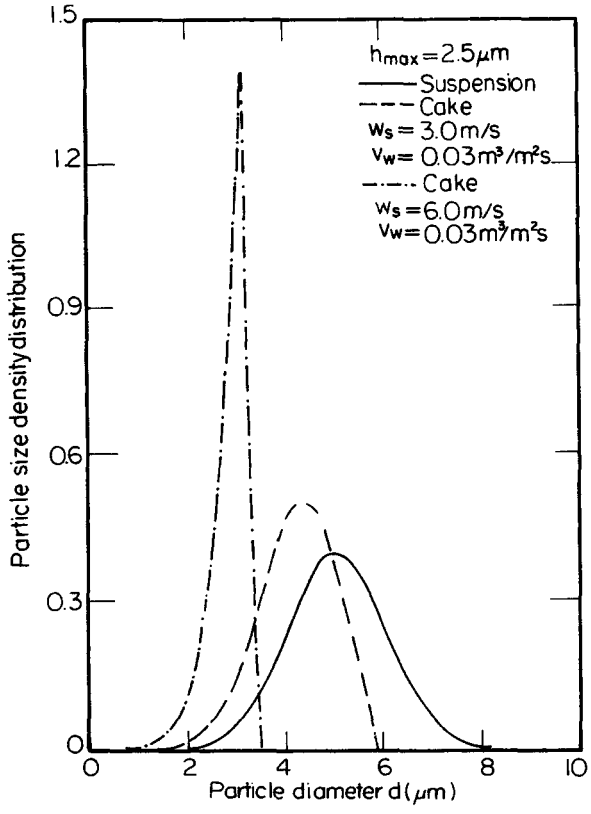

Figure 8b. Size distribution functions of suspended particles and cake particles permeation fluxes.

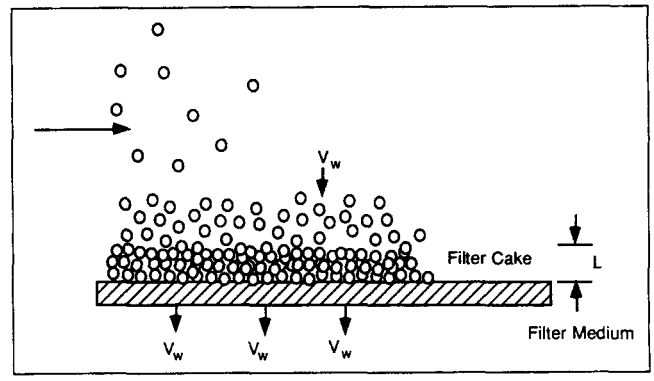

Figure 9. Cake formation in cross-flow filtration.

conditions under which this assumption holds and the procedure one may apply when such an assumption is not valid will be discussed later.)

First, let us assume that the suspension to be filtered is monodispersed and the cake formed is incompressible. For an incompressible cake, the liquid velocity across the cake at any instant is constant (and independent of the position within the cake). If L denotes the cake thickness, the rate of cake growth, dL/dt, is:

$$\frac{dL}{dt}=\frac{\epsilon_{so}v_w}{\epsilon_s-\epsilon_{so}}\gamma \tag{19}$$

where ϵ_{so} is the solidosity (volume fraction of particles) of the suspension and ϵ_s is the solidosity of the cake formed. γ is the fraction of the particles transported to the membrane surface which achieved deposition. For polydispersed suspension, γ should be replaced by $\bar{\gamma}$ of Eq. 17.

The instantaneous permeation velocity, v_w, is:

$$v_w=\frac{k}{\mu}\frac{P^o-P_o}{L+L_o} \tag{20}$$

and

$$L_o=k\frac{\Delta x_m}{k_m} \tag{21}$$

where k is the cake permeability, k_m the permeability of the membrane, and Δx_m the membrane thickness. P^o is the pressure of the suspension and P_o, the pressure at the downstream side of the membrane.

Equations 19 through 21 together with Eq. 16 (or Eq. 17 for polydispersed suspensions) and the initial condition, $L=0$ at $t=0$, are the governing equations for cross-flow filtration if the filter cake formed is incompressible. These equations can best be solved numerically since the adhesion probability, γ (or $\bar{\gamma}$), depends upon v_w in a rather involved manner. The numerical solution gives both the permeation flux, v_w, and the cake thickness, L, as functions of time.

The results of the incompressible cake case given above can be extended to the compressible cake case in the following manner. The permeability, k, and solidosity, ϵ_s, of a compressible cake are functions of the compressive stress to which

the cake is subject, P_s. The constitutive equations relating k and ϵ_s with P_s may be written as:

$$\epsilon_s = \epsilon_s^o \left(1 + \frac{P_s}{P_a}\right)^{\beta} \tag{22a}$$

$$k = k_o \left(1 + \frac{P_s}{P_a}\right)^{-\delta} \tag{22b}$$

where P_a, β, and δ are empirical parameters. ϵ_s^o and k_o are the solidosity and permeability values at the zero-stress state. If the membrane surface (or, therefore, the slurry/cake interface) is planar (or with negligible curvature effect), one has:

$$P_l + P_s = P^o \tag{23}$$

where P_l is the pressure of the liquid in the pore space of the cake.

For compressible cakes, the cake growth rate can also be found from Eq. 19 by replacing ϵ_s with ϵ_{sav}, the average cake solidosity. The cake growth rate becomes:

$$\frac{dL}{dt} = \frac{\gamma \epsilon_{so}}{\epsilon_{sav} - \epsilon_{so}} v_w \tag{24}$$

For polydispersed suspensions, γ should be replaced by $\bar{\gamma}$, and the average solidosity, ϵ_{sav}, is defined as (Stamatakis, 1990):

$$\epsilon_{sav} = \frac{\int_o^{P_{sm}} k \epsilon_s dP_s}{\int_o^{P_{sm}} k dP_s}. \tag{25}$$

where P_{sm} is the compressive stress value at the upstream side of the membrane surface.

Substituting the constitutive relationship of Eqs. 22a and 22b into Eq. 25, ϵ_{sav} is found to be:

$$\epsilon_{sav} = \epsilon_s^o \left(\frac{1-\delta}{1-\delta+\beta}\right) \frac{(1+\pi_{sm})^{1-\delta+\beta} - 1}{(1+\pi_{sm})^{1-\delta} - 1} \tag{26}$$

and

$$\pi_{sm} = P_{sm}/P_a \tag{27}$$

As before, the permeation flux, v_w, may be assumed to be constant across the cake at any instant. For compressible cake, Eq. 20 may be modified to give:

$$v_w = \frac{k_{av}}{\mu} \frac{P^o - P_{lm}}{L} = \frac{k_m (P_{lm} - P_o)}{\mu \Delta x_m} \tag{28}$$

where k_{av} is the average cake permeability. P_{lm} is the liquid pressure at the upstream side of the membrane. k_{av} is given as (Stamatakis, 1990):

$$k_{av} = k_o \frac{(1+\pi_{sm})^{1-\delta} - 1}{\pi_{sm}^{(1-\delta)}} \tag{29}$$

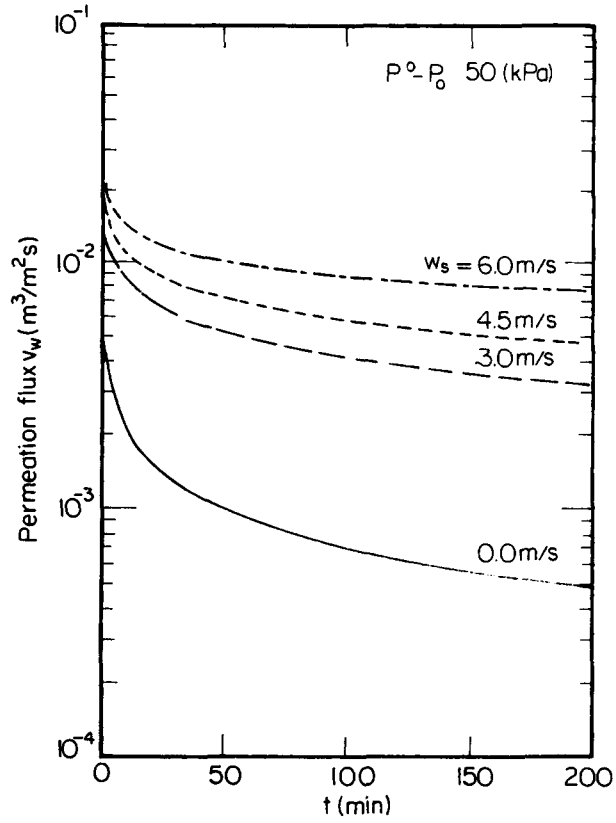

Figure 10. Permeation flux vs. time for various cross-flow velocities, $P^o - P_o = 50$ kPa (incompressible-cake case).

Similar to the incompressible-cake case, the solution of Eqs. 24 and 28 with the initial condition of zero cake thickness at $t = 0$ gives the performance of cross-flow filtration. In carrying out the numerical integration, one must use a trial and error procedure in order to find the value of $P_{sm} (= P^o - p_{lm})$ from Eq. 28. The trial and error procedure is necessary since k_{av} is now a function of P_{sm}.

Sample Simulation Results and Discussion

Certain simulation results are presented here to illustrate the models described above. The suspension was assumed to be monodispersed, and the physical properties of the suspension and those of the cake are listed in Table 1. It was assumed that the suspension flows in a slit formed by two parallel walls at a distance of 15 mm, having a small part of the total channel length permeable (of the order of 10^{-2} m) on one of the parallel walls, a configuration similar to that used by Fischer and Raasch (1986) in their experimental study.

The simulation results for the incompressible-cake case are shown in Figures 10 and 11. The results were obtained by numerically integrating Eq. 19 with the initial condition that $L = 0$ at $t = 0$ by an integration package (EPISODE). The permeation flux is given as a function of time at an operating pressure of 50 kPa. The model predicts an initially large decrease in permeation flux followed by a more gradual decline. The effect of the cross-flow velocity becomes more pronounced as time increases; an increase in cross-flow velocity w_s results

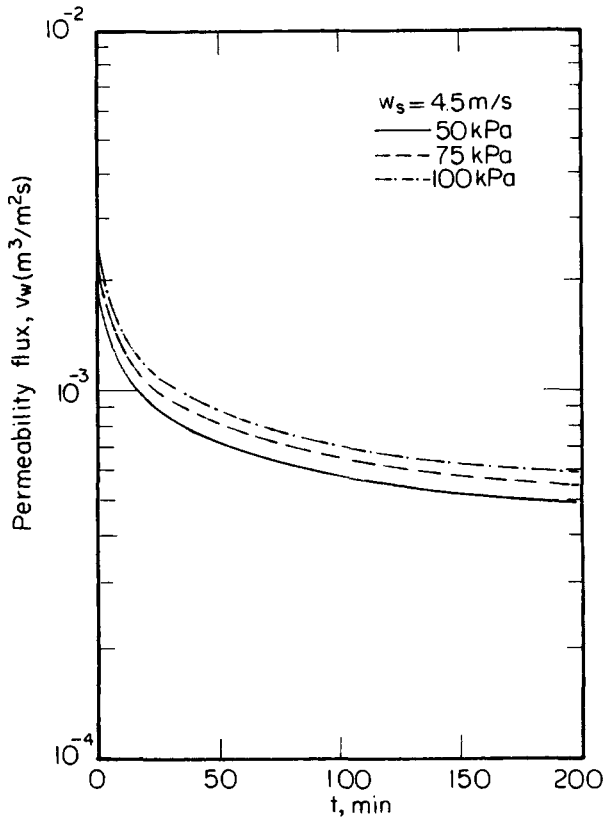

Figure 11. Permeation flux vs. time for various pressure drops (incompressible-cake case).

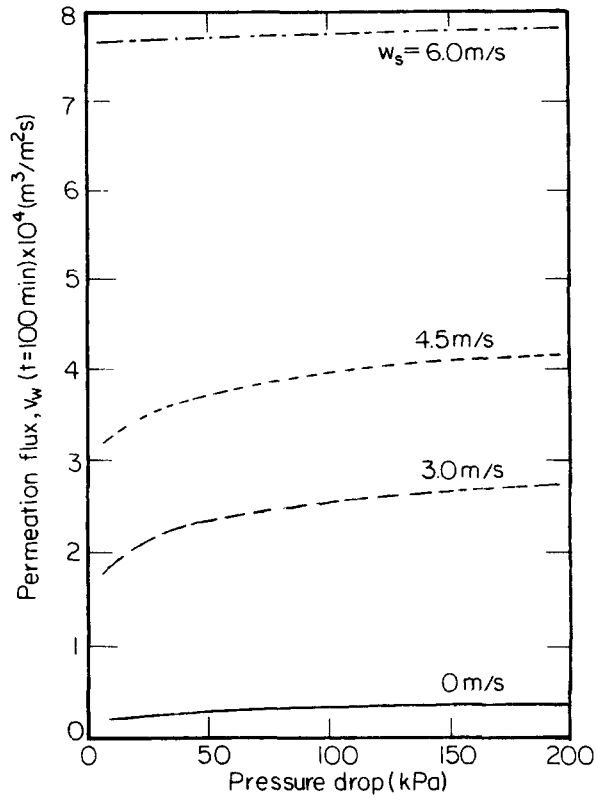

Figure 12a. Permeation flux vs. pressure drop at time $t = 100$ min, for different cross-flow velocities (incompressible-cake case).

in an increase in permeation flux. The influence of pressure drop across the slurry and the permeable walls can be seen more clearly by cross-plotting the results of Figure 10. In Figure 11, the permeation flux was plotted as a function of time for different pressure drops, that is, 50 kPa, 75 kPa, and 100 kPa, while the cross-flow velocity was kept constant at 4.5 m/s. As expected, the permeation flux increases as the pressure drop increases.

The results of the compressible-cake case are given in Figures 12 and 13. These results were obtained by integrating Eqs. 24 and 28. The constitutive relations of the cake are those of Eqs. 22a and 22b, with $\beta = 0.1$, $\delta = 0.8$, and $P_a = 1$ kPa. Figure 12 demonstrates the dependence of the permeation velocity, v_w, on the applied pressure drop, $P^o - P_o$, corresponding to different values of w_s at $t = 100$ min and 200 min. The increase in v_w due to the increase in the applied pressure drop is relatively small, a conclusion which was obtained independently by Fischer and Raasch (1986) and Murkes and Carlsson (1988) in their respective experimental studies.

In Figure 13 is shown the cake thickness as a function of time corresponding to different values of w_s and $P^o - P_o = 50$ kPa. Increasing the cross-flow velocity decreases the cake growth rate, although the cake thickness is always a monotonically increasing function of time. The cake growth rate is initially large but diminishes in the later stage of filtration. The maximum value of cake thickness in these figures was of the order of 1 mm. Since the distance between the parallel walls was 15 mm and the permeation flux was small, the cross-flow velocity remained nearly constant, a condition which was assumed in the calculations.

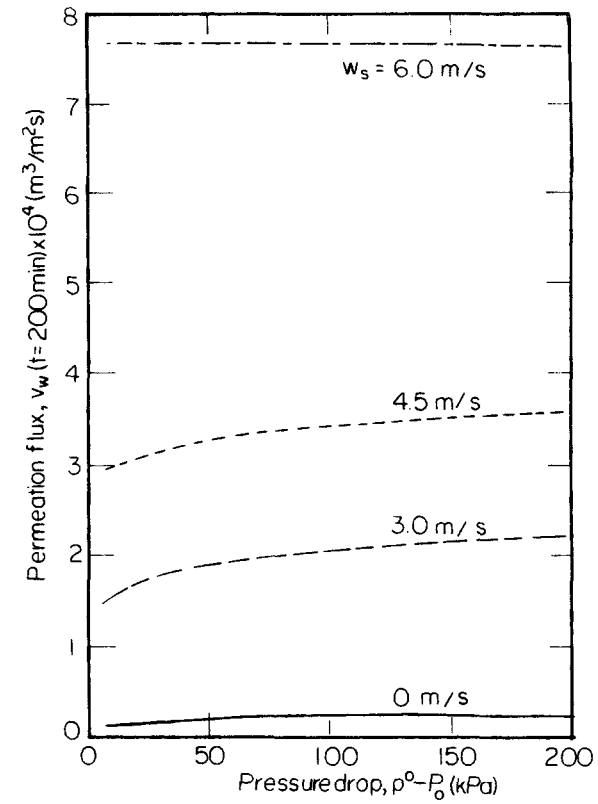

Figure 12b. Permeation flux vs. pressure drop at time $t = 200$ min, for different cross-flow velocities (incompressible-cake case).

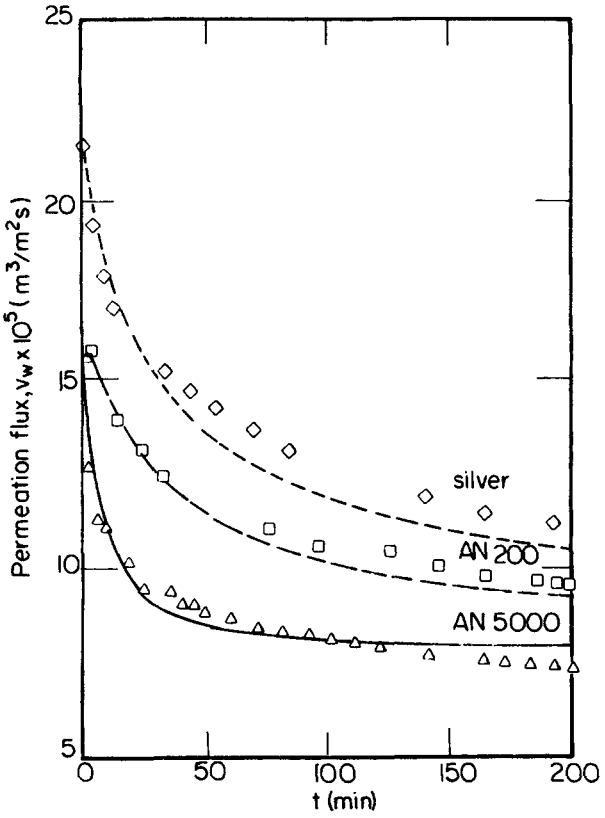

Figure 13. Permeation flux decline data: Murker and Carlsson (1991) vs. present model.

Additional calculations were made to demonstrate the capability of the present model to describe experimental results of cross-flow filtration. Murkes and Carlsson (1988) collected experimental data of permeation flux vs. time for different microporous membranes. The suspension and cake properties used in their experiments are given in Table 2. The microporous membranes used in the experiments included silver (0.5 μm) metallic membrane and Gelman Acropor AN200 (0.2 μm) and AN5000 (5.0 μm) polymeric membranes. Assuming that the suspensions of finely dispersed kaolin used by Murkes and Carlsson may be approximated as monodispersed suspensions and the cake formed was incompressible, Eqs. 19 and 20 were used together with an optimization-search procedure to obtain the cake solidosity, ϵ_s, and permeability, k. Furthermore, for a specific membrane, the medium equivalent cake thickness, L_o, was estimated using the reported initial permeation flux value. The values of ϵ_s and k obtained from the optimization-search procedure are included in Table 2. In turn, based on the determined k and ϵ_s values, the variation of v_w with time was predicted from Eqs. 19 and 20 and compared with the experimental data of Murkes, as shown in Figure 13.

From the results shown above, it is clear that our model is capable of predicting the three main features of cross-flow membrane filtration; (a) the rapid flux decline initially, (b) the diminishing rate of flux decline as time increases, and (c) the enrichment of fine particles on cake formation. The comparisons shown in Figure 13 indicate that the model represents experimental data with sufficient accuracy. Although ϵ_s and k of the model may be considered as adjustable parameters, the values of ϵ_s and k used in model predictions are consistent with their respective physical significance. In other words, the values of ϵ_s and k for the three cases of Figure 13 (which are listed in Table 2) are of the same order of magnitude of the ϵ_s and k values of filter cakes composed of Kaolin particles according to the data compiled by Shirato et al. (1987). This fact therefore should add credence to the validity of the model.

The fact that three different sets of ϵ_s and k values were used for the same type of filter cake can be attributed to the differences in the size distribution of the deposited particles of the three experiments. As discussed before, reducing permeation flux results in the formation of cakes composed of finer particles. The permeation flux shown in Figure 13 decreased in approximately the same order as the permeability was reduced from silver to AN5000 membranes. Thus, the variation of the estimated values of permeability and solidosity with the permeation flux from silver to AN5000 membranes is in agreement with the previously mentioned predictions.

The model formulation and sample simulations results given above assumed that the permeation flux, cake thickness and suspension solidosity do not vary longitudinally. The condition under which this assumption is valid may be found as follows. Consider a channel composed of two parallel membranes separated at a distance of 2b. The inlet suspension has a solidosity of ϵ_{so} and enters the channel at a velocity of w_s. The solidosity of the suspension at a distance of x from the inlet, by mass balance, can be found to be:

$$\epsilon_{s|x} = \frac{w_s \epsilon_{so} b - \epsilon_s x \dfrac{dL}{dt}}{w_s b - v_w x} = \frac{w_s \epsilon_{so} b}{w_s b - v_w x} = \frac{\epsilon_{so}}{1 - \dfrac{v_w x}{w_s b}} \tag{29}$$

since the cake growth rate diminishes with time. The condition that $\epsilon_{s|x}$ is approximately the same as ϵ_{so} requires that:

$$\frac{v_w x}{w_s b} \ll 1 \tag{30}$$

In most practical applications of cross-flow filtration, v_w is of the order 10^{-4} m/s while w_s is of the order of 1 m/s. b may vary from 10^{-3} to 10^{-2} m. The above requirement is met if the longitudinal distance is of the order of 1 m or less. For

Table 2. Physical Properties of Slurry and Cake of Finely Dispersed and Stabilized Kaolin, Murkes and Carlsson (1988)

Parameters	Microporous Membranes		
	Silver	AN200	AN5000
ϵ_{so}	0.0033	0.0033	0.0033
d_p	1 μm	1 μm	1 μm
ρ_l	1,000 kg/m^3	1,000 kg/m^3	1,000 kg/m^3
ρ_s	2,658 kg/m^3	2,658 kg/m^3	2,658 kg/m^3
μ	0.001 Pa·s	0.001 Pa·s	0.001 Pa·s
w_s	2.5 m/s	2.5 m/s	2.5 m/s
ϵ_{so}^*	0.121	0.127	0.1937
k_o	0.940×10^{-15} m^2	0.472×10^{-15} m^2	0.4267×10^{-16} m^2
L_o	0.873×10^{-4} m	0.596×10^{-4} m	0.546×10^{-5} m
P^o	20 kPa	20 kPa	20 kPa

*Obtained by parameter search in this study.

cases where the requirement of Eq. 30 is not met, it is necessary to divide the channel into a number of sections of such length that they satisfy the condition given by Eq. 30. One can then apply Eqs. 19 and 20 (or Eqs. 24 and 28) to each of these sections, with the inlet solidosity value of each section calculated from Eq. 29.

Acknowledgment

This study was performed under the Grant No. CBT 86-17260 "Particle Deposition in Membrane Processes," National Science Foundation.

Notation

C_i = volume fraction of the ith type particle of the suspension
d = equivalent diameter of membrane channel
d_p = particle diameter
$\overline{d_p}$ = mean value of d_p
d_{p_i} = diameter of the ith type particle
F_p = force acting on a particle along the main flow direction
F_q = force acting on a particle along the permeation direction
$F_{q_1}, F_{q_2}, F_{q_3}$ = forces given by Eqs. 6, 8 and 9, respectively
f = friction factor
h = protrusion height
h_{max} = maximum value of h
h_{min} = minimum value of h necessary for deposition
k = cake permeability
k_{av} = average value of k
k_m = medium permeability
k_o = cake permeability at zero stress (see Eq. 22a)
L = cake thickness
L_o = defined by Eq. 21
N = total of particle types
P = probability
P_a = parameter of the constitutive equations (Eqs. 22a and 22b)
p_l = liquid pressure
P^o = pressure of the suspension
P_o = pressure on the downstream side of the medium
p_s = compressive stress
P_{lm} = pressure at the medium surface
p_{sm} = compressive stress at the medium surface
Re = Reynolds number, defined as $d\, w_s \rho_l / \mu$
t = time
u_L = liquid velocity
v_w = permeation flux (velocity)
w = liquid velocity along the medium surface
w_s = cross-flow velocity
x_i = volume fraction of the total population of particles present in the suspension with diameter d_{p_i}
y = distance away from the medium surface
y_i = volume fraction of particles with diameter d_{p_i} in the cake

Greek letters

β = exponent of Eq. 22a
γ = adhesion probability
γ_i = adhesion probability of particles with diameter d_{p_i}
$\overline{\gamma}$ = fraction of particles deposited, defined by Eq. 17
Δx_m = medium thickness
δ = exponent of Eq. 22b
ϵ_s = cake solidosity
ϵ_{so} = volume fraction of particles of suspension
ϵ_{sav} = average ϵ_s defined by Eq. 25
ϵ_s^o = volume of ϵ_s at zero stress state
μ = liquid viscosity
ν = kinematic viscosity of liquid
ρ_l = liquid density
ρ_s = particle density
π_{sm} = defined as P_{sm}/P_a

Literature Cited

Altena, F. W., and G. Belfort, "Lateral Migration of Spherical Particles in Porous Channel Flow," *Chem. Eng. Sci.*, **39**, 343 (1984).
Blatt, W. F., A. David, A. S. Michaels, and L. Nelson, "Solute Polarization and Cake Formation in Membrane Ultrafiltration: Causes, Consequence and Control Techniques," in *Membrane Science and Technology*, J. E. Flinn, ed., Plenum Press, New York, pp. 47–67 (1970).
Davis, R. H.., and S. A. Birdsell, "Hydrodynamic Model and Experiments for Crossflow Microfiltration," *Chem. Eng. Commun.*, **49**, 217 (1987).
Davis, R. H., and D. T. Leighton, "Shear-Induced Transport of a Particle Layer Along a Porous Wall," *Chem. Eng. Sci.*, **42**, 275 (1987).
Drew, D. A., J. A. Schonberg, and G. Belfort, "Lateral Inertial Migration of a Small Sphere in Fast Laminar Flow through a Membrane Duct," *Chem. Eng. Sci.*, **46**, 3219 (1990).
Fischer, E., and J. Raasch, "Model Tests of the Particle Deposition at the Filter-Medium in Cross-Flow Filtration," 4th World Filtration Congress Proc. Part II, pp. 9.9-9.16 (1986).
Henry, J. D., "Cross Flow Filtration," in *Recent Developments in Separation Science*, **2**, N. N. Li, ed., pp. 205–225, CRC Press, Cleveland, OH (1972).
Lu, W.-M., and S.-C. Ju, "Selective Particle Deposition in Crossflow Filtration," *Sep. Sci. Technol.*, **24**, 517 (1989).
Murkes, J., and C. G. Carlsson, *Cross Flow Filtration: Theory and Practice*, John Wiley & Sons, New York (1988).
O'Neill, M. E., "A Sphere in Contact with a Plane While in a Slow Linear Shear Flow," *Chem. Eng. Sci.*, **23**, 1387 (1968).
Porter, M. C., "Concentration Polarization with Membrane Ultrafiltration," *Ing. Eng. Chem. Prod. Res. Dev.*, **11**, 234 (1972).
Romero, C. A., and R. H. Davis, "Global Model of Crossflow Microfiltration based on Hydrodynamic Particle Diffusion," *J. Membrane Sci.*, **39**, 157 (1988).
Romero, C. A., and R. H. Davis, "Transient Model of Crossflow Microfiltration," *Chem. Eng. Sci.*, **45**, 13 (1990).
Schonberg, J. A., and E. J. Hinch, "Inertial Migration of Spheres in Poiseuille Flow," *J. Fluid Mech.*, **167**, 415 (1986).
Shirato, M., T. Murase, E. Iritani, T. A. Tiller, and A. F. Alciatore, "Filtration in the Chemical Process Industry," in *Filtration-Principles and Practices*, 2nd ed., M. J. Matteson and C. Orr, eds., Marcel Dekker, New York (1987).
Stamatakis, K., "Analysis of Cake Formation and Growth in Liquid-Solid Separations," PhD Dissertation, Syracuse University, Syracuse, NY (1990).
Vasseur, P., and R. G. Cox, "The Lateral Migration of Spherical Particle in Two Dimensional Shear Flow," *J. Fluid Mech.*, **78**, 385 (1976).
Zydney, A. L., "Crossflow Membrane Plasmapheresis—An Analysis of Flux and Hemolysis," D.Sc. Dissertation, Massachusetts Institute of Technology, Cambridge, MA (1985).
Zydney, A. L., and C. K. Colton, "A Concentration Polarization Model for the Filtrate Flux in Cross-Flow Microfiltration of Particulate Suspensions," *Chem. Eng. Commun.*, **47**, 1 (1986).

Manuscript received Oct. 7, 1991, and revision received Dec. 11, 1992.